J Mol Model (2008) 14:171–181
DOI 10.1007/s00894-007-0259-7

ORIGINAL PAPER

DFT tests for group 8 transition metal carbonyl complexes

Pipsa Hirva · Matti Haukka · Minna Jakonen · M. Andreina Moreno

Received: 4 October 2007 / Accepted: 29 November 2007 / Published online: 5 January 2008
© Springer-Verlag 2007

Abstract The applicability of several popular density functionals in predicting the geometrical parameters and energetics of transition metal carbonyl complexes of iron, ruthenium and osmium has been studied. The methods tested include pure GGA functionals (BLYP, BP86, OPBE, HCTH, PBE, VSXC) and hybrid GGA functionals (B3PW91, B3LYP, PBE1PBE, MPW1K, B97-2, B1B95, PBE1KCIS). The effect of changing the metal basis set from Huzinaga's all-electron basis to SDD scECP basis was also studied. The results show, that hybrid functionals are needed in order to describe the back-bonding ability of the carbonyl ligands as well as to deal with metal-metal bonds. The best general performance, when also the computational cost was considered, was obtained with hybrid functionals B3PW91 and PBE1PBE, which therefore provide an efficient tool for solving problems involving large or medium sized transition metal carbonyl compounds.

Keywords Density functional calculations · Iron · Osmium · Ruthenium · Transition metals

Introduction

Carbonyl containing transition metal complexes is a widely used class of compounds with various applications especially in catalytic chemistry. While the experimental techniques in synthesis and analysis of transition metal complexes have been developed during the past decades, computational studies have only recently been routinely accessed, mainly because of the development of more accurate density functional methods. However, the field of transition metal carbonyl complexes is still lacking a systematic study on the performance of the numerous functionals and basis sets available for today's computational chemist. On the other hand, a generally applicable method is not easy to find among the functionals, because the performance of density functional methods can not be systematically improved by improving the level of theory in the same way as the traditional ab initio methods. Very accurate and detailed benchmark studies with small organic or organometallic species provide valuable information on the performance of different methods and basis sets, but important limitations are often faced when the problem includes medium or large size transition metal compounds. A compromise between the accuracy of the method/basis set and the complexity of the system is normally required in a search for a general purpose method applicable for wider range of compounds.

Previous studies on the applicability of DFT functionals have mainly been concerned on small organic molecules. Exhaustive benchmark studies by Zhao et al. for developing databases to test different DFT methods in evaluating atomization energies, barrier heights and non-bonding interactions provide a good example of such work [1–4]. It should be noted, that the latest functional developments of the Truhlar's group (M05, M06-L) [5–7] have been shown to perform well in the tests for small transition metal compounds. A large number of modern DFT functionals have also been tested in different hydrogen abstraction or addition reactions of small organic molecules [8]. Additionally, trends in the R-X bond dissociation energies (R = Me, Et, i-Pr, t-But; X = H, CH_3, OCH_3, OH, F) have been computed utilizing various density functionals [9].

Among transition metals, the work on the performance of different functionals has focussed more on the particular problem than a general application of DFT methods. A recent study from Furche and Perdew describes tests for several

P. Hirva (✉) · M. Haukka · M. Jakonen · M. A. Moreno
Department of Chemistry, University of Joensuu,
P.O. Box 111, FI-80101 Joensuu, Finland
e-mail: pipsa.hirva@joensuu.fi

popular functionals in *3d* transition metal compounds [10]. Various functionals have been compared in the detailed analysis of vibrational frequencies in $M(CO)_n$ compounds [11], nuclear shielding constants and chemical shifts for first-row transition metal complexes [12], hyperfine coupling constants for Cu and V complexes [13], metal-metal bonding in binuclear transition metal complexes [14], and proton affinities and gas phase basicities of biologically interesting phosphates and phosphoranes [15]. Accurate M-CO interactions have been obtained by testing different methods for Pd_nCO (n=1,2) species [16]. Typical study on transition metal carbonyl complexes utilizes only one or two DFT methods without systematic testing of the methods. Examples of such studies are evaluation of the first dissociation energy of the $M(CO)_n$ compounds [17–19], or the dissociation energy of the heteroligand L in $M(CO)_nL$ [17, 18]. Core-electron binding energies of first row transition metal carbonyls and nitrosyls have also been calculated by BP86 functional [20]. More specific problems with transition metals include predicting redox potentials for first row transition metal ions in water [21], DFT tests for electronic transition energies in $CuCl_2$ [22], and the performance of different functionals for estimating prototype reaction profiles with palladium [23].

Because of the lack of systematic information concerning the general applicability of current popular and easily available density functionals, both pure and hybrid functionals, in calculating the properties of late transition metal carbonyl complexes, we launched a comparative study on several types of compounds that we have been working with during the past years. The compounds used in this work were mono- or trinuclear carbonyl complexes of Fe, Ru and Os, including pentacarbonyls $[M(CO)_5]$, cluster compounds $[M_3(CO)_{12}]$, and mononuclear complexes with bipyridine ligands $[RuClH(bpy)(CO)_2]$ and $[Ru(SCN)_2(bpy)(CO)_2]$. Additionally, decarbonylation energies were calculated for $[M(bpy)(CO)_2Cl_2]$. In the complexes, the reliable description of the metal-carbonyl back-bonding and the metal-metal bonds has been found to be the key element of the correct structural and electronic properties. This paper aims to shed light on advantages and limitations of different functionals in calculations involving large and medium sized Fe, Ru and Os carbonyl compounds.

Computational details

All calculations were carried out with the Gaussian03 program package [24]. DFT level of theory with several currently widely utilized functionals, both pure gradient corrected DFT and non-local hybrid density functionals, summarized in Table 1, were selected for the quantum chemical studies. Instead of aiming to detailed benchmarking of the numerous available DFT methods, the selection of the functionals was based on the popularity of them in different applications. The basis set comprised of quasi-relativistic Stuttgart-Dresden effective small core potential [25] augmented with an extra p-polarization function for the *4d* and *5d* metal atoms (SDD(p)), (exponents Ru: 0.081, Os: 0.077) [26] and a standard all-electron basis set 6–31G* for other atoms. The inclusion of larger ligand basis sets (6–311 + G(d) or cc-pVQZ) was also investigated for the pentacarbonyl compounds. The results obtained with the ECP basis were compared with the Huzinaga's all-electron (AE) basis set [26]. Full optimization from the same initial geometry with all the functionals was performed for each of the complexes. No symmetry restrictions were applied in the calculations.

Table 1 Classification of the functionals tested in this study

GGA	meta-GGA	hybrid GGA	hybrid meta-GGA
HCTH	VSXC	B3PW91	B1B95
PBE		B3LYP	PBE1KCIS
BLYP		PBE1PBE	
BP86		MPW1K	
OPBE		B97-2	

Results and discussion

Pentacarbonyl compounds

Iron, ruthenium and osmium form relatively stable pentacarbonyls, which exhibit a trigonal bipyramide structure with three equatorial and two axial carbonyls (Fig. 1). The optimized M-C bond distances compared to the available experimental data are shown in Fig. 2.

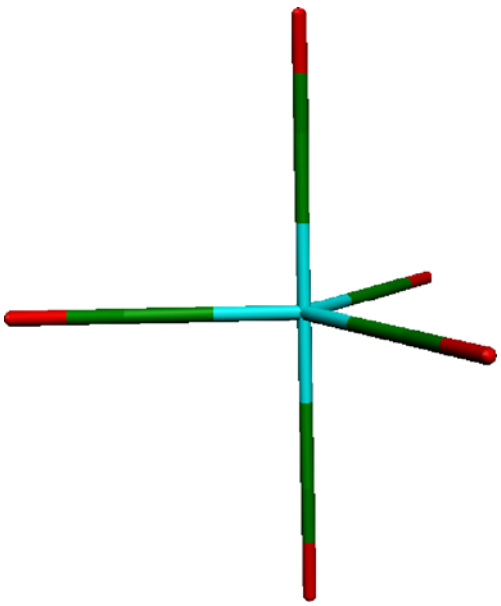

Fig. 1 The structure of $M(CO)_5$ complexes, M = Fe, Ru, Os

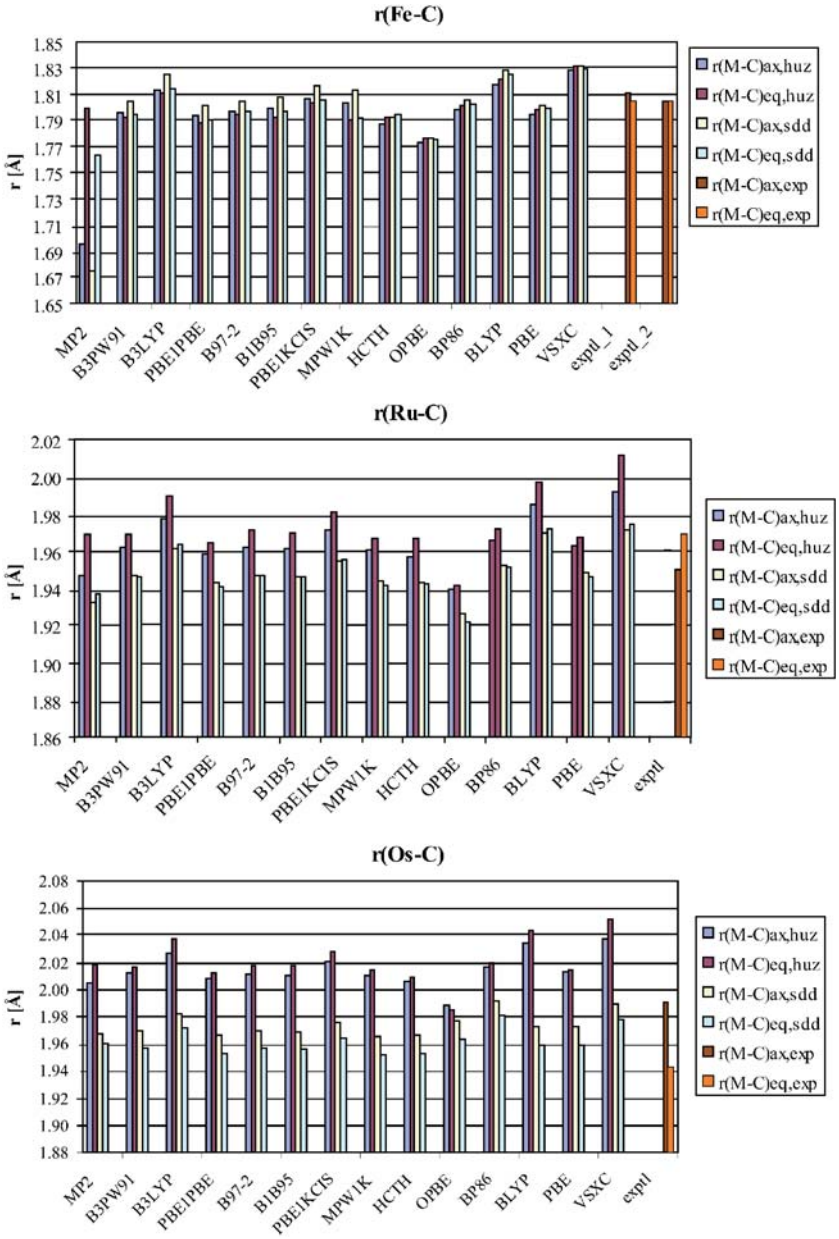

Fig. 2 Optimized M-C bond distances [Å] for pentacarbonyl compounds of Fe, Ru and Os, calculated with different density functionals and MP2 method. Experimental data: Fe [27(R= 3.0%),28(R=1.9%)], Ru [29] and Os [30]

As a first observation, the basis set dependence is different for the *3d*, *4d* and *5d* transition metals, resulting from the different requirements for relativistic effects. Ruthenium pentacarbonyl is very well described with the non-relativistic Huzinaga's all-electron basis set, whereas in iron pentacarbonyl there is an underestimation of the Fe-C bond length with most of the functionals, and in osmium pentacarbonyl the M-C bond distance is considerably overestimated. Not surprisingly, the quasi-relativistic Stuttgard-Dresden ECP basis set performs much better with the osmium compound than the non-relativistic Huzinaga basis. Futhermore, compared to the all-electron basis set, the frozen core approximation in the SDD basis yields notable CPU time savings especially for the heavier *5d* transition metals.

The trend in the CPU time required to fully optimize the structures is more or less the same for all pentacarbonyl complexes. The hybrid meta-GGA functionals were about 20% slower than the first generation functionals (B3PW91, B3LYP), yet they do not seem to considerably improve the accuracy for this type of complexes. Among the two basis sets tested, SDD was slightly slower for iron and slightly faster for ruthenium and osmium than the Huzinaga's all electron split valence basis in most cases. This can be rationalized by comparing the nature of the basis set for different metals. For iron, the SDD basis set uses a larger valence basis than Huzinaga's AE basis set, and the core part is relatively small for the first row transition metals. On the other hand, ruthenium and especially osmium have a

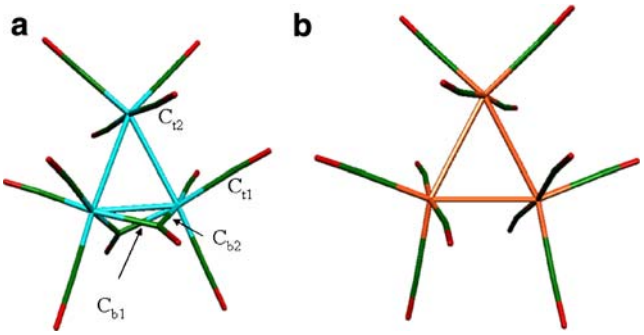

Fig. 3 Structure of the trinuclear metal carbonyl clusters $M_3(CO)_{12}$. **a**) M = Fe, **b**) M = Ru or Os. The corresponding labeling scheme of the carbonyls is used in Fig. 5. C_{t1} = terminal carbonyl, in=plane; C_{t2} = terminal carbonyl, off-plane, C_{b1} and C_{b2} = bridged carbonyls

larger amount of core electrons, and therefore the frozen core approximation can be more effectively utilized.

Most of the hybrid functionals give experimentally comparable results for the geometrical parameters of the transition metal pentacarbonyls, except B3LYP, which seems to overestimate the M-C bond distance slightly more than the other hybrid functionals. Also, the pure functional VSXC performs poorly, at least when connected to Huzinaga's basis set. For comparison, MP2 fails to reproduce the experimental structure of iron pentacarbonyl, but for ruthenium and osmium the results are similar with the DFT methods.

In iron pentacarbonyl, there is a similar overestimation of the carbonyl C-O bond lengths with most of the functionals. The most accurate C-O distances are produced by MPW1K functional, irregardless of the metal basis set. Pure func-

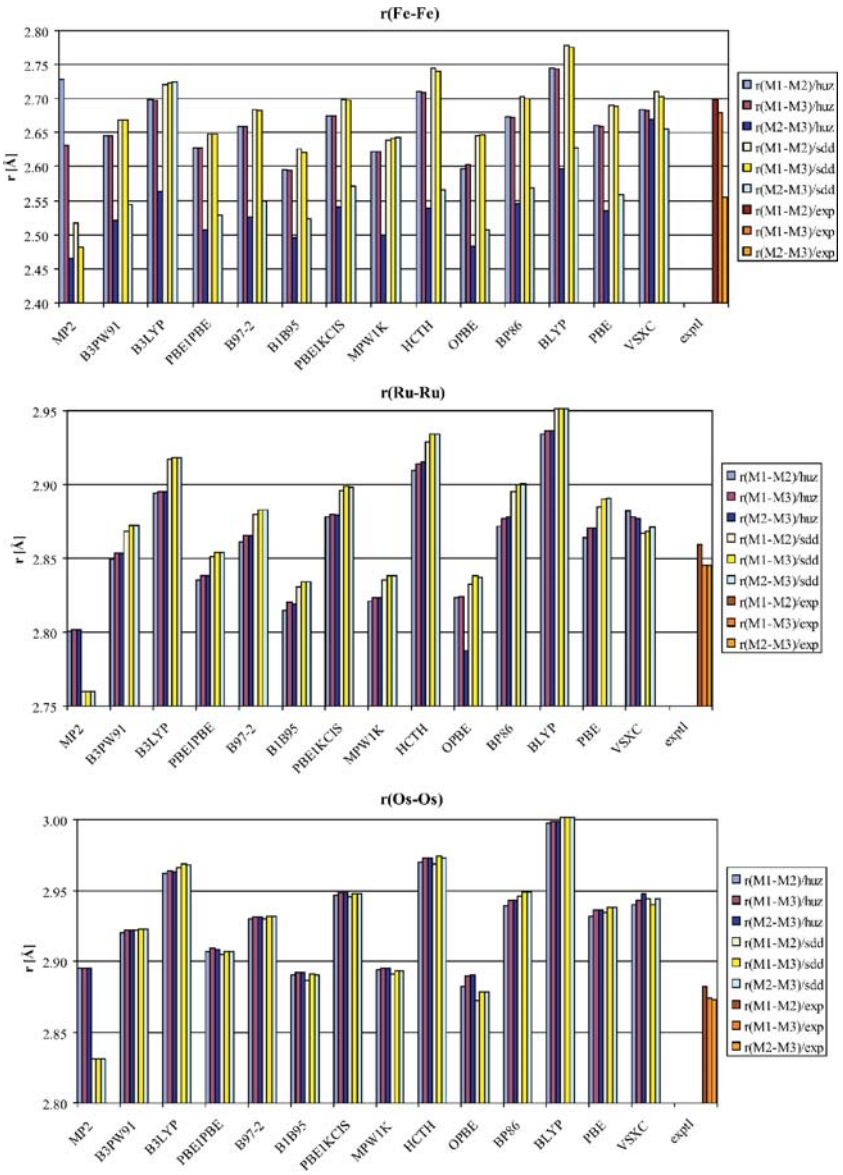

Fig. 4 Comparison of the M-M bond lenghts in $M_3(CO)_{12}$ clusters of iron, ruthenium and osmium calculated with different DFT functionals and MP2 method. Experimental X-ray data: Fe [31 (R=6.02%)], Ru [32 (R=3.2%)] and Os [33 (R=3.35%)]

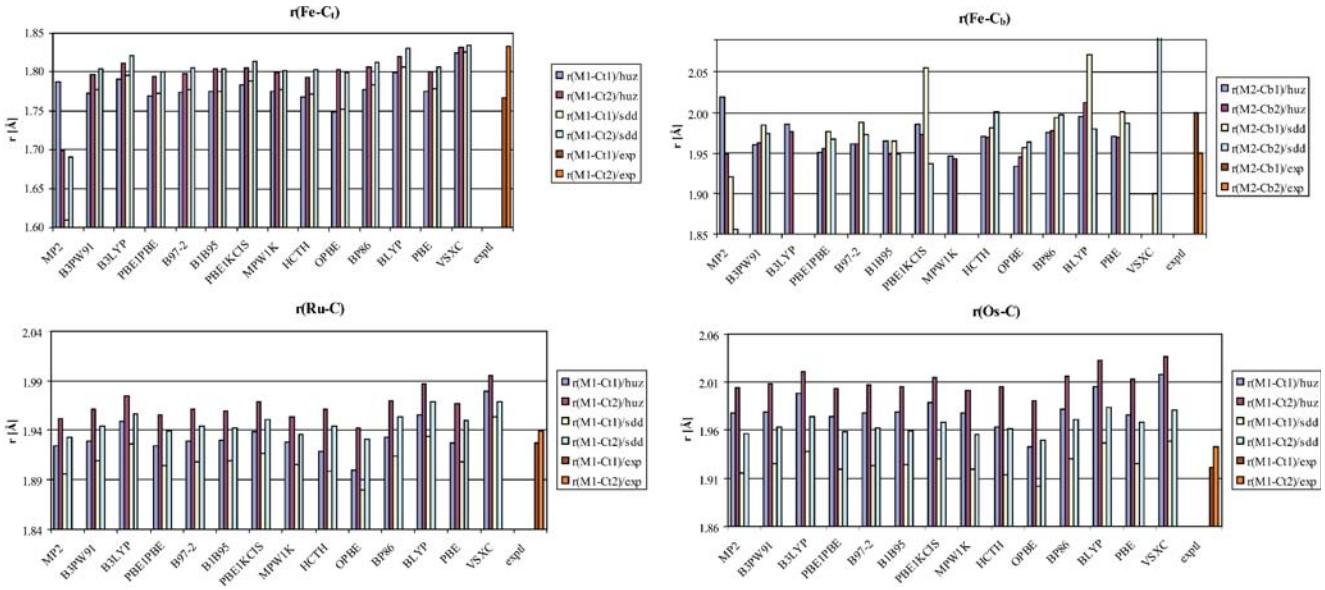

Fig. 5 Comparison of the M-C bond lenghts in $M_3(CO)_{12}$ clusters of iron, ruthenium and osmium calculated with different DFT functionals and MP2 method. Experimental data: Fe [31], Ru [32] and Os [33]

tionals seem to overestimate the distance more than the hybrid functionals. However, with ruthenium and osmium pentacarbonyls, the hybrid functionals reproduce the C-O bond lengths accurately, except for MPW1K, which underestimates the distance. Also with the heavier pentacarbonyls, the carbonyl bond length is overestimated more with the pure functionals. Obviously, the moderate size ligand basis set 6–31G(d) has an effect on the overestimation. Enhancing the ligand basis set to 6–311 + G(d) decreased the C-O bond length by 0.01Å, but it also doubled the required computational time. When a larger basis set cc-pVQZ was used for the ligands, the effect on the C-O bond lengths was the same, but a 40 times longer CPU time was required to optimize the compounds. Therefore, for practical applications with medium or large size transition metal compounds, the standard basis set 6–31G(d) should give geometrical parameters comparable to experiments. It should be noted, that the overestimation of the carbonyl bond length is even more pronounced with the MP2 method, which indicates that MP2 level of theory is incapable of describing the back-bonding of the carbonyl ligand and hence, is not recommended for metal carbonyl complexes.

It seems to be difficult to reliably describe the relative difference between the axial and equatorial bond distances. The difference depends more on the selection of the basis set than on the selection of the functional, at least among the hybrid functionals. For iron and ruthenium pentacarbonyls, Huzinaga's basis set gives differences more comparable to experiments. For osmium pentacarbonyl, better results are obtained with the SDD basis set. However, for gaseous pentacarbonyls, the experimental structures, obtained by low-temperature X-ray diffraction for iron complex [27, 28] and by electron diffraction for ruthenium [29] and osmium [30] complexes, might not be accurate enough to make a reliable estimation of these subtle geometrical effects. The trends within different functionals can, nevertheless, give information for the selection of the computational methods.

Trinuclear carbonyl clusters

Trinuclear carbonyl clusters such as $M_3(CO)_{12}$ of iron, ruthenium and osmium are well known catalyst precursors

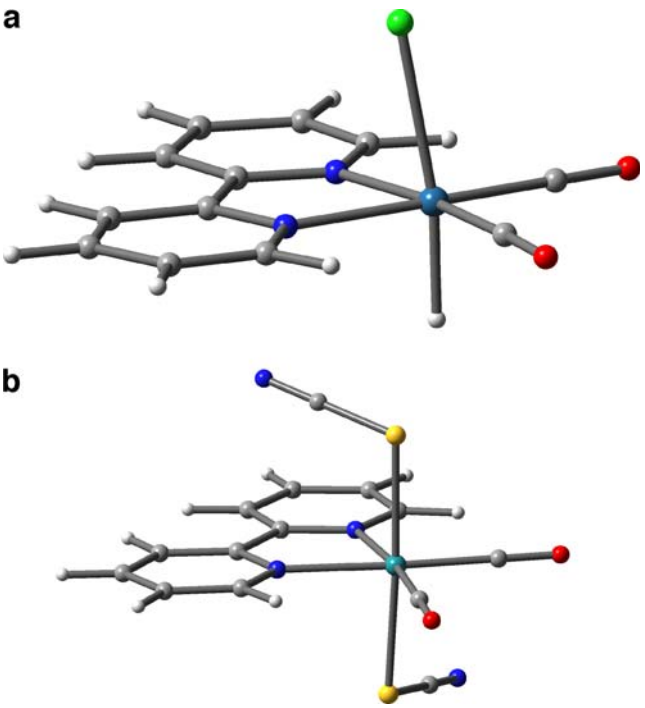

Fig. 6 The structure of selected bipyridine complexes, **a**) [RuClH(bpy)$(CO)_2$], **b**) [$Ru(SCN)_2$(bpy)$(CO)_2$]

and therefore experimentally widely studied. The trinuclear clusters of ruthenium and osmium have a similar structure with only terminal carbonyl ligands, whereas $Fe_3(CO)_{12}$ has two asymmetric carbonyl bridges at one edge of the cluster (Fig. 3). In the cluster compounds, there are two difficult bonding types, the metal-metal bond and especially the bridged carbonyl bonds, where an accurate description of the structure is important. The results of the DFT tests for

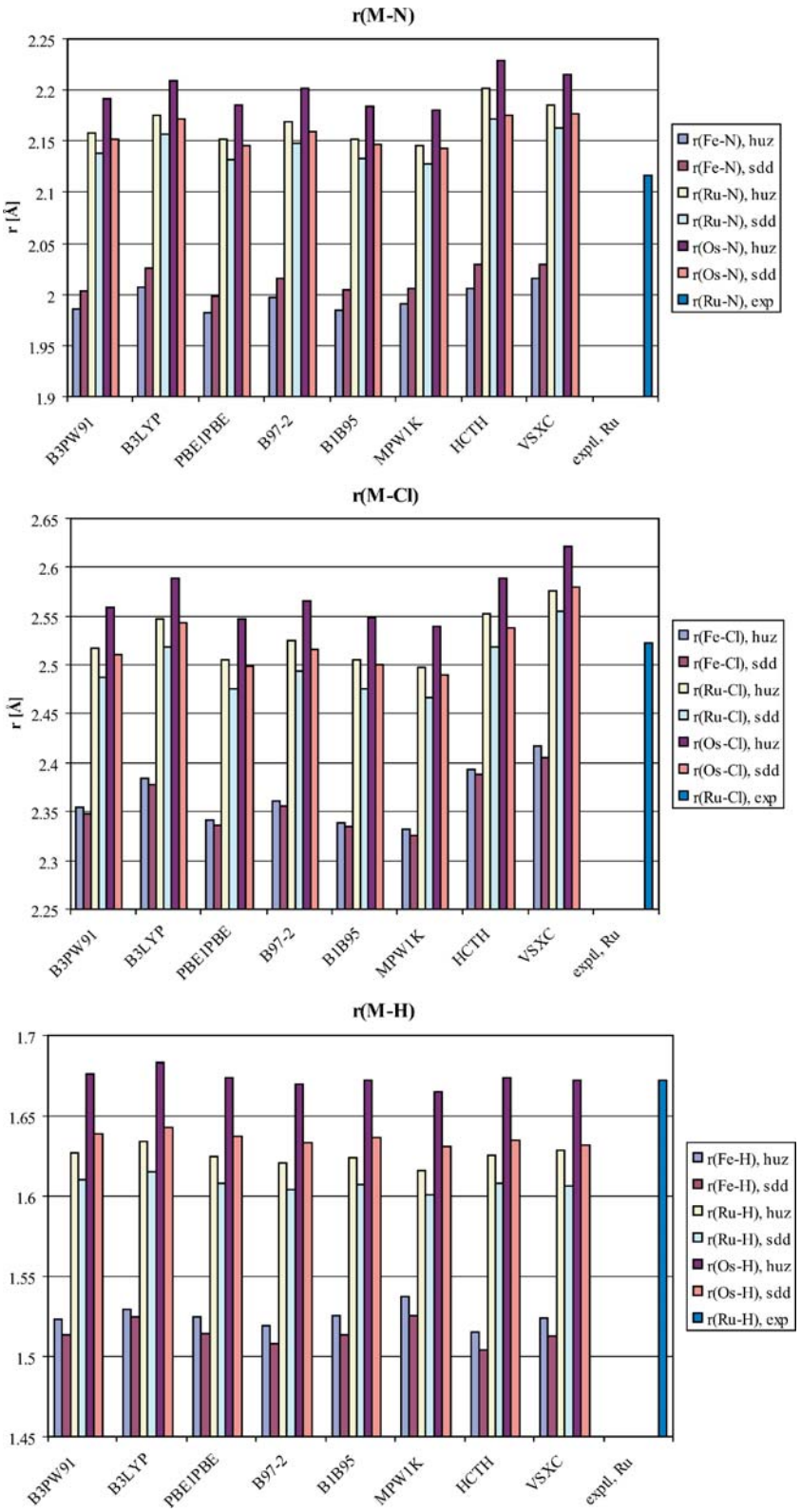

Fig. 7 Selected optimized parameters [Å] for the [MClH(bpy)$(CO)_2$] complex, M = Fe, Ru,Os, with different density functionals and basis sets. Experimental structure of [RuClH(bpy)$(CO)_2$] is taken from ref. [34 (R=2.57%)]

the fully optimized clusters are presented in Fig. 4 and Fig. 5.

Since $Fe_3(CO)_{12}$ cluster has two asymmetric bridging carbonyls, the Fe-Fe bond lengths are not identical, but there are one shorter (M2–M3 in Fig. 4) and two longer bonds (M1–M2 and M1–M3). This overall structure is reproduced with most of the methods, except with B3LYP/SDD, MPW1K/SDD, VSXC/SDD and VSXC/Huz, which where unable to describe the bridged carbonyls, and exhibited only terminal carbonyl ligands. Consequently, with these functionals the Fe-Fe bond lengths are similar. It should be noted, that the experimental asymmetric nature of the bridges, where $r(Fe\text{-}C_{b1}) \neq r(Fe\text{-}C_{b2})$, could be better described by using the SDD basis set, since the Huzinaga's all-electron basis tended to optimize symmetrical bridges. The results for B1B95 and OPBE were poor within the Huzinaga's basis set because of the large underestimation of the M-M bond distance. With other hybrid functionals, SDD gives slightly more accurate bond distances for iron. The same applies for the Fe-C bond distances, most accurate results can be adopted by using the hybrid GGA functionals with SDD basis set.

In the case of $Fe_3(CO)_{12}$, notable improvement on the geometry of the bridged carbonyls was obtained, when the ligand basis set was extended to 6–311 + G(d). When this basis set was used together with the SDD basis set for iron, PBE1PBE functional was able to reproduce the correct structure of the two asymmetric bridging carbonyls. The

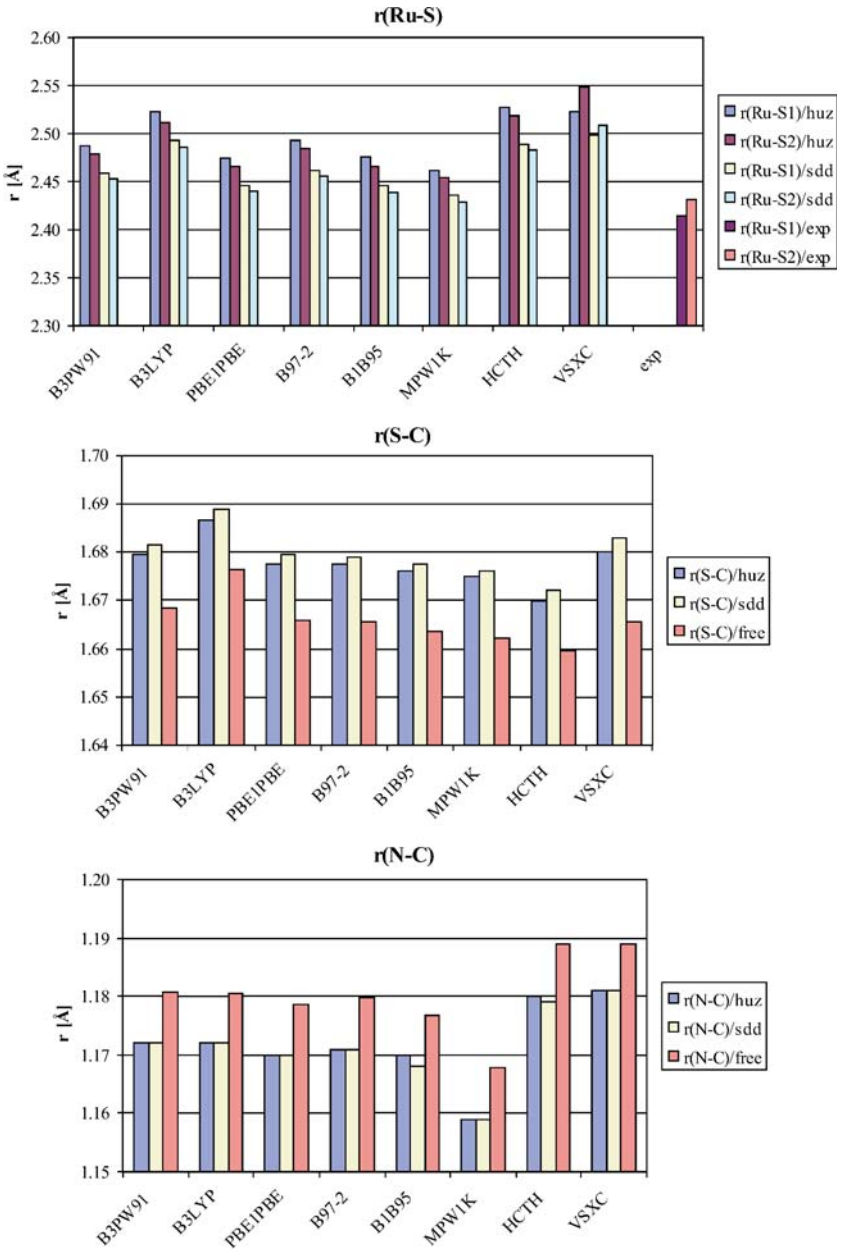

Fig. 8 Computational parameters for $[Ru(SCN)_2(bpy)(CO)_2]$ complex compared to experimental values and optimized parameters for free thiocyanate. Experimental structure has been adopted from ref. [35 (R= 5.07%)]

result indicates, that for trinuclear clusters with bridging carbonyl ligands, the ligand basis set should be extended at least to triple-zeta quality, which will mean increased computational requirements. The effect on the terminal carbonyls was much smaller; hence ruthenium and osmium clusters were accurately calculated also with the 6–31G(d) ligand basis set.

MP2 method completely failed to reproduce the experimental structure of $Fe_3(CO)_{12}$ with both basis sets. The optimized structure had only one asymmetric bridge with the Huzinaga AE basis, and the remaining terminal carbonyls showed a twisted geometry with a large variety of bond distances. In Fig. 5 we have shown the average bond distance for the Fe-C_t bond. Even though the MP2/SDD method was able to reproduce two asymmetric bridging carbonyls, the Fe-Fe bond distance was too short, especially between the bridges, and consequently the C-O distance was very much overestimated.

Generally, the results for ruthenium and osmium carbonyl clusters where similar with all the functionals studied here. Pure functionals BLYP, BP86, VSXC and HCTH, and the hybrid functional B3LYP overestimated the metal-metal distance more than the other functionals. For ruthenium, the best results were obtained with the hybrid functionals B3PW91, PBE1PBE and B97-2, which have been widely used for predicting the properties of ruthenium complexes. For osmium, new hybrid functionals B1B95 and MPW1K gave more accurate structures. Since both trinuclear ruthenium and osmium clusters have only terminal carbonyl ligands, the metal-carbon bond distances were generally quite well obtained. Only the pure functional VSXC clearly failed to reproduce the correct metal-carbon bonds, not only because of the large overestimation of the bond length, but also because of the large distortion of the M-C-O angle from the optimum, nearly 180° value. It should be noted, that for both clusters, all the functionals predicted a staggered conformation of the carbonyl ligands, while the experimental crystal structure shows an eclipsed conformation, which is, however, most probably due to the packing effects in solid state and can not be reproduced by single molecule calculations.

In contrast to the iron carbonyl cluster, the overall structure of ruthenium and osmium clusters was correctly obtained by MP2 method. However, the metal-metal bond distance was again underestimated and the C-O distance was heavily overestimated. An additional disadvantage in using the MP2 method is the larger computational requirements of the calculations; in the case of trinuclear clusters the required CPU time was 10–20 times longer than with most of the density functional methods.

Bipyridine complexes

Transition metal complexes with heteroaromatic ligands belong also to a very important group of organometallic compounds. They have been frequently utilized as catalysts, light-sensitive compounds and synthetic precursors. We selected two different types of compounds shown in Fig. 6 including bipyridine as bidentate nitrogen ligand. The hydride and thiocyanate ligands were chosen because they represent different types of bonds in the complexes, which allowed us to test further the performance of the various density functional methods. Because MP2 method gave less accurate geometrical parameters in the earlier tests, especially for the carbonyl ligands, it was not studied here. The results for the selected geometrical parameters can be found in Figs. 7 and 8.

Although the experimental hydride structure is available only for ruthenium [34], structural trends can be expected to be similar for the corresponding osmium complex. Also, the tests should reveal the relative differences between the methods studied here. When the geometry of the ruthenium complex is compared with the experimental values, several trends can be obtained: the Ru-N bonding distance of the bipyridine ligand is generally overestimated by 0.02–0.05 Å, except for functionals B3LYP, HCTH and VSXC, where the overestimation is larger. Also generally the SDD basis set gives slightly better Ru-N distances than the Huzinaga basis. The basis set dependence is different for iron complexes than for ruthenium and osmium: SDD yields longer Fe-N distances than Huzinaga. All the functionals are able to reproduce symmetrical binding of the two

Table 2 Relative decarbonylation energies [kJ mol^{-1}] of the [M(bpy)$(CO)_2Cl_2$] complexes with M = Fe, Ru and Os

	ΔE(Fe), huz	ΔE(Fe), sdd	ΔE(Ru), huz	ΔE(Ru), sdd	ΔE(Os), huz	ΔE(Os), sdd
B3PW91	130.9	122.4	180.9	195.8	202.1	229.7
B3LYP	118.1	109.4	171.6	185.1	218.9	217.8
PBE1PBE	137.9	130.3	190.6	207.0	212.6	246.3
B97-2	119.9	111.5	171.1	187.7	193.1	223.9
B1B95	127.6	119.6	188.1	196.2	202.0	230.7
MPW1K	124.1	98.3	174.3	192.7	203.9	238.0
HCTH	130.8	131.3	166.8	183.6	185.5	215.6
VSXC	185.1	177.0	202.7	218.1	215.2	238.0

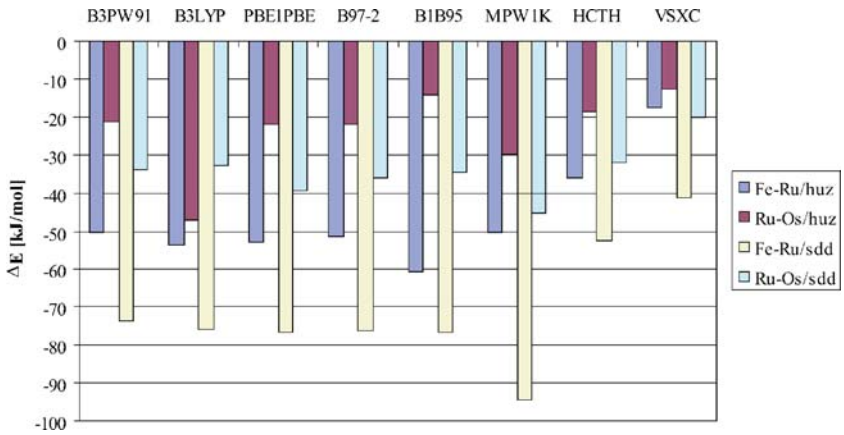

Fig. 9 The difference in decarbonylation energies between iron and ruthenium as well as between ruthenium and osmium complexes

nitrogens of the bipyridine ligand, which is also obtained in the experimental structure.

There is larger variation in the results for M-Cl distance. Generally, for ruthenium the Huzinaga basis set performs better, resulting from the larger underestimation of the M-Cl distance with the SDD basis set. However, since some of the functionals tend to overestimate the distance, there is a fortuitous compensation of errors with, for example, the B3LYP/SDD combination, which yields very accurately the experimental value.

The M-H bond distance seems to be especially problematic for all functionals, and consequently the distance is largely underestimated, compared to the experimental value of 1.67 (3) Å in the ruthenium complex. However, variation between different functionals is small even with the pure functionals, which suggests that there might be difficulties in obtaining the experimental location of the hydride ligand, as well.

To study the effect of different *trans*-ligands in the similar bipyridine complex, we chose to compute the optimized geometrical parameters of $[Ru(SCN)_2(bpy)(CO)_2]$, which are shown in Fig. 8. Also here the only experimental structure is for ruthenium complex [35].

Again, nearly all the functionals predict the overall geometry more or less correctly. The only exception is the pure functional VSXC, which leads to a heavily distorted geometry. All the functionals overestimate the Ru-S bond lengths, and the overestimation is more severe with B3LYP, HCTH and VSXC. Also in this case, use of SDD basis set on the metal improves the accuracy compared to the experimental structure.

We studied the effect of complexation in the SCN ligand geometry by comparing it with the computational results of free isolated SCN molecule (Figs. 8b and c). The results show lengthening of the S-C bond and shortening of the N-C bond upon complexation. The amount of the change in the bond lengths is very similar with all functionals, even if the actual distances vary somewhat depending on the method. The change in the metal basis set also has a very small effect in the ligand geometry.

Decarbonylation reactions

In catalysis, one of the initial steps in the reaction routes is often the dissociation of one or more of the carbonyl ligands, when transition metal carbonyl complexes are utilized as catalysts. Therefore, it is interesting to know, how different functionals perform in the comparison of relative decarbonylation energies. We chose an apparently simple decarbonylation reaction of $[M(bpy)(CO)_2Cl_2]$. However, the calculation of full reaction energy profile would have been too time-consuming for the testing purposes, thus we chose to calculate only the relative energies of stable, ground state reactants and products in the reaction (1)

$$M(bpy)(CO)_2Cl_2 \rightarrow M(bpy)(CO)Cl_2 + CO \quad (1)$$

The relative decarbonylation energies for M = Fe, Ru, and Os are presented in Table 2.

All the methods studied here gave a similar trend for the decarbonylation energies, even though the actual energy values show considerable variation in some cases. The required energy to remove one carbonyl ligand from the $[M(bpy)(CO)_2Cl_2]$ complex follows the order Fe <Os, which indicates, that it is much easier to decarbonylate an iron complex than ruthenium or osmium. More clearly this can be seen, when the difference in the decarbonylation energies is compared (Fig. 9).

Table 3 The difference in the decarbonylation energies [kJ mol^{-1}] of $[M(bpy)(CO)_2Cl_2]$ calculated with Huzinaga's AE basis set (huz) and Stuttgart&Dresden scECP basis set (sdd) with M = Fe, Ru or Os

	diff(huz-sdd) Fe	diff(huz-sdd) Ru	diff(huz-sdd) Os
B3PW91	8.5	−14.9	−27.6
B3LYP	8.8	−13.6	1.1
PBE1PBE	7.6	−16.4	−33.7
B97-2	8.4	−16.6	−30.8
B1B95	8.0	−8.2	−28.6
MPW1K	25.9	−18.5	−34.1
HCTH	−0.5	−16.8	−30.0
VSXC	8.1	−15.4	−22.9

The energy difference is much larger between iron and ruthenium complexes than between ruthenium and osmium. The difference is even more pronounced when relativistic effects are accounted for with the SDD basis set. On the other hand, most of the functionals give a rather constant difference, with the exception of pure functionals, which predict a smaller effect of the central metal atom on the decarbonylation energies. The difference between the relativistic and non-relativistic calculations is also quite constant for most functionals, as can be seen in Table 3.

The difference between the two basis sets becomes larger with heavier transition metal elements, obviously as a result of the larger relativistic effects, which the Huzinaga's basis set does not account for. Nevertheless, as long as the difference is known, also the otherwise very stable Huzinaga's basis set can be used, since it does predict a qualitatively correct picture.

In the reaction (1), the decarbonylated product M(bpy)$(CO)Cl_2$ is formally a 16-electron complex, and can in principle have a triplet ground state. For the iron compound, the triplet state was found at lower energy than the singlet state with all the functionals, contrary to ruthenium and osmium complexes, which adopted a singlet ground state. Since all the tested functionals showed the same behaviour, the resulting decarbonylation energies followed the same trends with the singlet state calculations, and therefore only the singlet state calculations are reported here in detail. Full optimization of the spin state was not in the scope of the current study, since here we aimed to investigate the similarities and differences between the tested functionals.

Conclusions

It is always difficult to give any definite recommendations to which functional and basis set to use because of the large variation of the results. Also, accurate benchmarking of the methods with very small molecules does not always reflect the special structural or electronic features of medium and large size compounds utilized in practical applications. Therefore, it will be crucial to examine carefully the applicability of different computational options each time a new type of transition metal complexes is adopted in the studies. In the current work, we selected several popular density functional methods with two different types of basis sets in order to study the basic geometrical and energetic properties of group 8 transition metal carbonyl complexes.

Our results show, that within the selected functionals, the best performance can be obtained with the hybrid functionals. The pure functionals cannot describe the difficult bonding of the carbonyl ligands, especially the bridged ones. However, with the hybrid GGA functionals there are in most cases only slight differences, and the first generation hybrid functionals can work as well and also faster than the second and third generation functionals. The best overall performance, considering also the relative computational requirements, were found with hybrid functionals B3PW91 and PBE1PBE, therefore providing an efficient tool for solving problems involving large or medium sized transition metal carbonyl compounds.

Among the two selected basis sets, the Huzinaga's AE basis and the Stuttgart-Dresden scECP basis set, in most complexes better geometrical parameters were obtained with the SDD basis set, especially for iron and osmium compounds. However, for ruthenium complexes, the very stable Huzinaga's all-electron basis set was found to produce reasonably reliable geometries. The standard 6–31G(d) basis set was found to be suitable for most of the ligands, except for bridged carbonyl ligands in the trinuclear iron cluster, where the ligand basis set of at least triple-zeta quality was required.

Even if the tests show less accuracy for a particular method or basis set, as long as the relative errors and limitations are known, it is often more convenient to use the same method that has been used in earlier studies. This way it will be easier to compare previous results on the current studies. The knowledge on the performance of current methods will enable one to make a necessary compromise between the computational requirements and the desired accuracy of the results.

Acknowledgements Financial support from the Academy of Finland (P.H., M.J.) is gratefully acknowledged.

References

1. Zhao Y, Pu J, Lynch BJ, Truhlar DG (2004) Phys Chem Chem Phys 6:673–676
2. Zhao Y, Gonzales-Garcia N, Truhlar DG (2005) J Phys Chem A 109:2012–2018
3. Zhao Y, Truhlar DG (2005) J Chem Theory Comput 1:415–432
4. Zheng J, Zhao Y, Truhlar DG (2007) J Chem Theory Comput 3:569–582
5. Zhao Y, Truhlar DG (2006) J Chem Phys 124:224105/1–6
6. Zhao Y, Schultz NE, Truhlar DG (2006) J Chem Theory Comput 2:364–382
7. Zhao Y, Truhlar DG (2006) J Chem Phys 125:194101/1–18
8. Andersson S, Grüning M (2004) J Phys Chem A 108:7621–7636
9. Izgorodina EI, Coote ML, Radom L (2005) J Phys Chem A 109:7558–7566
10. Furche F, Perdew JP (2006) J Chem Phys 124:044103/1–27
11. Jonas V, Thiel W (1995) J Chem Phys 102:8474–8484
12. Wilson PJ, Amos RD, Handy NC (2000) Phys Chem Chem Phys 2:187–194
13. Saladino AC, Larsen SC (2005) Catal Today 105:122–133
14. Petrie S, Stranger R (2004) Inorg Chem 43:2597–2610
15. Range K, Riccardi D, Cui Q, Elstner M, York DM (2005) Phys Chem Chem Phys 7:3070–3079

16. Schultz NE, Gherman BF, Cramer CJ, Truhlar DG (2006) J Phys Chem B 110:24030–24046
17. Hyla-Kryspin I, Grimme S (2004) Organometallics 23:5581–5592
18. van Wüllen C (1996) J Chem Phys 105:5485–5493
19. Ziegler T, Tschinke V, Ursenbach C (1987) J Am Chem Soc 109:4825–4837
20. Hu C-H, Chong DP (1996) Chem Phys Lett 262:733–736
21. Uudsemaa M, Tamm T (2003) J Phys Chem A 107:9997–10003
22. Ramirez-Solis A, Poteau R, Vela A, Daudey JP (2005) J Chem Phys 122:164306/1–10
23. Quintal MM, Karton A, Iron MA, Boese AD, Martin JML (2006) J Phys Chem A 110:709–716
24. Frisch MJ, Trucks GW, Schlegel HB, Scuseria GE, Robb MA, Cheeseman JR, Montgomery JA, Vreven T, Kudin KN, Burant JC, Millam JM, Iyengar SS, Tomasi J, Barone V, Mennucci B, Cossi M, Scalmani G, Rega N, Petersson GA, Nakatsuji H, Hada M, Ehara M, Toyota K, Fukuda R, Hasegawa J, Ishida M, Nakajima T, Honda Y, Kitao O, Nakai H, Klene M, Li X, Knox JE, Hratchian HP, Cross JB, Adamo C, Jaramillo J, Gomperts R, Stratmann E, Yazyev O, Austin AJ, Cammi R, Pomelli C, Ochterski JW, Ayala PY, Morokuma K, Voth GA, Salvador P, Dannenberg JJ, Zakrzewski VG, Dapprich S, Daniels AD, Strain MC, Farkas O, Malick DK, Rabuck AD, Raghavachari K, Foresman JB, Ortiz JV, Cui Q, Baboul AG, Clifford S, Cioslowski J, Stefanov BB, Liu G, Liashenko A, Piskorz P, Komaromi I, Martin RL, Fox DJ, Keith T, Al-Laham MA, Peng CY, Nanayakkara A, Challacombe M, Gill PMW, Johnson B, Chen W, Wong MW, Gonzales C, Pople JA (2004) Gaussian 03, Revision C.02. Gaussian Inc, Wallingford CT
25. Basis Sets were obtained from the Extensible Computational Chemistry Environment Basis Set Database, Version 02/02/06, as developed and distributed by the Molecular Science Computing Facility, Environmental and Molecular Sciences Laboratory which is part of the Pacific Northwest Laboratory, P.O. Box 999, Richland, Washington 99352, USA, and funded by the U.S. Department of Energy. The Pacific Northwest Laboratory is a Multi-Program Laboratory operated by Battelle Memorial Institute for the U.S. Department of Energy under contract DE-AC06-76RLO 1830. Contact Karen Schuchardt for further information. (2007)
26. Huzinaga S (ed.) (1984) Gaussian Basis Sets for Molecular Calculations. Physical Sciences Data 16, Elsevier, Amsterdam
27. Boese R, Blaeser D (1990) Z Kristall 193:289–290
28. Braga D, Grepioni F, Orpen AG (1993) Organometallics 12:1481–1483
29. Huang J, Hedberg K, Davis HB, Pomeroy RK (1990) Inorg Chem 29:3923–3925
30. Huang J, Hedberg K, Pomeroy RK (1988) Organometallics 7:2049–2053
31. Farrugia LJ, Gillon AL, Braga D, Grepioni F (1999) Organometallics 18:5022–5033
32. Braga D, Grepioni F, Tedesco E, Dyson PJ, Martin CM, Johnson BFG (1995) Transition Metal Chemistry 20:615–624
33. Churchill MR, DeBoer BG (1977) Inorg Chem 16:878–884
34. Haukka M, Hirva P, Luukkanen S, Kallinen M, Ahlgren M, Pakkanen TA (1999) Inorg Chem 38:3182–3189
35. Homanen P, Haukka M, Pakkanen TA, Pursiainen J, Laitinen RH Organometallics 15:4081–4084